Effect of cyclosporin A on functional recovery in the spinal cord following contusion injury

Effect of cyclosporin A on functional recovery in the spinal cord following contusion injury

Siobhan S. McMahon,1,2 Silke Albermann, 2 Gemma E. Rooney, 2 Cathal Moran, 2 Jacqueline Hynes, 1 Yolanda Garcia, 1 Peter Dockery, 1 Timothy O'Brien, 2 Anthony J. Windebank 3 and Frank P. Barry 2

1, *Department of Anatomy, National University of Ireland, Galway, Ireland*
2, *Regenerative Medicine Institute, National University of Ireland, Galway, Ireland*
3, *Department of Neurology, Mayo Clinic, Rochester, MN, USA*

Correspondence:
Professor Frank Barry, Regenerative Medicine Institute, National Centre for Biomedical Engineering and Science, National University of Ireland Galway, Ireland. T: +353 91 495108, F: +353 91 495547.
E: frank.barry@nuigalway.ie

Abstract
Considerable evidence has shown that the immunosuppressant drug cyclosporin A (CsA) may have neuroprotective properties which can be exploited in the treatment of spinal cord injury. The aim of this study was to investigate the cellular environment within the spinal cord following injury and determine whether CsA has an effect on altering cellular interactions to promote a growth-permissive environment. CsA was administered to a group of rats 4 days after they endured a moderate contusion injury. Functional recovery was assessed using the Basso Beattie Bresnahan (BBB) locomotor rating scale at 3, 5 and 7 weeks post-injury. The rats were sacrificed 3 and 7 weeks post-injury and the spinal cords were sectioned, stained using histological and immunohistochemical methods and analysed. Using stereology, the lesion size and cellular environment in the CsA-treated and control groups was examined. Little difference in lesion volume was observed between the two groups. An improvement in functional recovery was observed within CsA-treated animals at 3 weeks. Although we did not see significant reduction in tissue damage, there were some notable differences in the proportion of individual cells contributing to the lesion. CsA administration may be used as a technique to control the cell population of the lesion, making it more permissive to neuronal regeneration once the ideal environment for regeneration and the effects of CsA administration at different time points post-injury have been identified.

Key words:
regeneration; glial scar; spinal cord injury; motor function; stereology.

Introduction

The extent of spinal cord injury varies between individuals,depending on the type of injury endured and the location of the injury in the spinal cord (Hulesbosch, 2002). The most common spinal cord injury is a contusion injury which damages the spinal cord due to the physical impact and also due to a period of secondary cellular degeneration which will eventually result in the formation of a glial scar around the injured region (Dietz & Curt, 2006).

Initially, neutrophils and macrophages migrate to the site of injury. The function of these immune cells is dependent on their position in relation to the injury and the time point following injury (Carlson et al. 1998).

Macrophages have been found to express iNOS, which plays a dominant role in producing nitric oxide (NO) after spinal cord injury (Diaz-Ruiz et al, 1999). Following injury, a reaction between NO and generates peroxynitrite, a reactive oxygen species that further contributes to lipid peroxidation (Diaz-Ruiz et al. 2005). This is proposed to be a major cause of post-traumatic cell damage and axonal demyelination following spinal cord injury (Ibarra et al. 2003).

The glial cell population is also stimulated to express cytokines. This increased expression of cytokines brings about a change in the structure and function of astrocytes to become reactive astrocytes. This results in the formation of a compacting glial scar around the perimeter of the lesion site. The expression of chondroitin sulfate proteoglycans (CSPGs) by a number of cell types within the glial scar has also been identified as an inhibitory factor to axonal regeneration (Fidler et al. 1999; Chen et al. 2002). Evidence of this lies in research carried out where the chondroitinase ABC (ChABC) enzyme was administered following spinal cord injury and reduced the inhibitory effect of many CSPGs such as neuroglycan 2 (NG2), versican, neurocan and brevican (Ikegami et al. 2005; Massey et al. 2008).

The current drug therapy approach in the treatment of spinal cord injury involves the administration of methylprednisolone (MP), which inhibits lipid peroxidation and reduces neuronal degeneration (Sayer et al. 2006; Anderberg et al. 2007). However, it is not recommended that MP be administered more than 8 h after the initial injury (Kwon et al. 2004). CsA is an immunosuppressive drug which has been shown to have neuroprotective properties similar to MP. CsA has been shown to exert its neuroprotective effect via calcineurin inhibition, its ability to reduce lipid peroxidation, blockade of mitochondrial permeability transition pore and neurotrophic factor release (Diaz-Ruiz et al. 1999, 2000, 2005; Clausen & Bullock, 2001; Sullivan et al. 2005; Ibarra & Diaz-Ruiz, 2006; Ibarra et al. 2007).

CsA exerts an anti-ischemic effect by delaying neuronal cell death in rat ischemia (Miyata et al. 2001; Yu et al. 2004; Yamaguchi et al. 2006). CsA also induces expression of the growth-associated protein-43 (GAP-43) involved in neuronal process extension (Lautermilch & Spitzer, 2000). Overall, one would expect CsA treatment to result in an increase in neurons and oligodendrocytes compared with untreated animals (Ibarra et al. 2003).

The aim of the present study was to determine the reaction of the injured spinal cord cellular environment at

the lesion site following treatment with CsA. Effect of CsA on lesion size and functional recovery was also assessed.

Materials and methods

Spinal cord injury

Twenty four female Sprague Dawley rats weighing approximately 220 g were used in this study. The rats were anaesthetized by intraperitoneal (IP) injection of ketamine and xylazine (100 mg kg and 10 mg kg, respectively) following which a laminectomy was performed at T8–T10 level. All animals received a 200 kdynes moderate contusion injury at T9 using an Infinite Horizon Impactor Device (Precision Systems and Instrumentation, Lexington, KY, USA). The wound was then closed with absorbable suture material (Vicryl, 4 metric). The animals were randomly divided into two groups: a CsA-treated group ($n = 12$) and a control group ($n = 12$). CsA (5 mg kg) was given subcutaneously to the CsA-treated group 4 days post-injury and every day thereafter for the duration of the experiment. Each animal received a subcutaneous injection of enrofloxacin antibiotic (5–10 mg kg) once daily for a minimum period of a week. Additional antimicrobial therapy was administered if signs of urinary tract infection were detected. Pain relief was provided by administering buprenorphine (Torbugesic) at a dose rate of 0.1–0.25 mg kg twice daily for 7 days after surgery. Saline solution (3.5 mL) was administered subcutaneously for 3 days following the surgery. The bladder was manually expressed twice daily from the day of injury. Both the control and the CsA-treated groups were subdivided into two groups, one group of CsA-treated and control animals were sacrificed 3 weeks post-injury and the other CsA and control group at 7 weeks post-injury. All animal experiments were conducted in accordance with local institutional and national regulations.

Behavioral analysis

Following injury, all animals were assessed using the BBB locomotor rating scale to determine their motor function. Animals had an average BBB score of 2 on the day following injury. All BBB scoring was performed blind by two trained examiners. Animals were analysed using BBB assessment on both left and right hindlimbs at 3 weeks, 5 weeks and 7 weeks post-injury. Mean BBB ± SE was calculated for each treatment and time point.

Tissue processing

Animals were deeply anaesthetized by IP injection of sodium pentabarbitone and perfused transcardially with saline followed by 4% paraformaldehyde in 0.1 M phosphate-buffered saline (PBS). A 2-cm-long piece of the injured thoracic region of the spinal cord was dissected out and postfixed overnight with 4% paraformaldehyde. Spinal cords were cryoprotected by immersion in 30% sucrose overnight and frozen in liquid nitrogen chilled isopentane. The spinal cords were cryosectioned transversely at 20um thickness in a rostral to caudal direction. Sampling regions, located at 300um intervals, were examined within each injured spinal cord. Approximately 35 sampling regions were collected per spinal cord through the centre of the injury. Eight spinal cord sections were collected at each sampling region and two sections were placed on each slide. The first of the four slides in each sampling region was rehydrated in PBS, mounted with anti-fading mounting media and coverslipped. These slides were used for stereological estimation of lesion size. The other slides in each sampling region were used for immunohistochemical, histological and scanning electron microscopical (SEM) analysis.

Immunohistochemical staining

Immunohistochemistry was carried out on five animals from each of the four groups, i.e. control and CsA-treated groups at 3 and 7 weeks post-injury. One slide, containing two sections, was immunostained with each primary antibody used in this study. Frozen sections were rehydrated in PBS and incubated with 20% normal goat serum (NGS) block solution in PBS containing 0.2% Triton X for 20 min. The primary antibodies (NeuN: Ms IgG, Chemicon, 1 : 100; myelin basic protein (MBP): rabbit polyclonal, Chemicon, 1 : 100; brain lipid binding protein (BLBP): rabbit polyclonal, Chemicon, 1 : 100; vimentin: Ms IgG, Sigma- Aldrich, 1 : 100; glial fibrillary acidic protein (GFAP): Rabbit Polyclonal, DakoCytomation, 1 : 300) were diluted in PBS containing 2% NGS + 0.02% Triton X. Sections were incubated in primary antibody for 2 h at room temperature. Sections were then washed three times in PBS. The corresponding secondary antibody, either tetramethyl rhodamine isothiocyanate (TRITC, Sigma-Aldrich) or fluorescein isothiocyanate (FITC, Sigma-Aldrich) was diluted 1 : 100 in PBS and incubated for 1 h at room temperature in darkness. Sections were again washed and counterstained with 1ug mL DAPI (Sigma) for 5 min. Following washing, a drop of anti-fading mounting medium was placed on each slide, which was then coverslipped. Double staining was performed on slides to minimize the amount of tissue used. A negative control was carried out for each antibody staining by substituting PBS for the primary antibody. Images were captured on an Olympus IX81 fluorescent microscope at 4 and 20 magnification. The 20 immunostained images were inverted and converted to grey scale using ADOBE PHOTOSHOP software to allow for easier identification of positively stained tissue.

Histology

One slide from each animal within the CsA-treated and untreated animals was stained using Masson's trichrome with Gomori's
aldehyde fuchsin to identify collagen. Images were captured at 2.5 ×and 20 on a Leitz DMRXE light microscope.

SEM

One slide from each animal within the CsA-treated and untreated group was processed for SEM. SEM was used to visualize the surface
features of the transverse sections of injured spinal cord. To prepare the cryosections for SEM, the cryosections were fixed in 1% osmium for 1 h, and dehydrated in alcohol and hexamethyl disilazine for 20 min. Cryosections were then air-dried and the region around
the sections was scored and snapped so that the samples could be mounted on carbon-painted stubs. Sections were gold-coated
with a sputter-coater at 30 mA for 4 min. Sections were visualized with a Hitachi 2600N SEM using an accelerating voltage of 20 kV.
Images were captured at 100 and 600
×
.

Stereology

Images of the first section of each sampling region of all four animals in both the control and the CsA-treated group were captured at
4 using a Nikon Eclipse E400 light microscope. These images were used in lesion volume estimation. Stereological analysis was carried
out to estimate the volume of the lesion created by the injury and the proportion of the spinal cord occupied by this lesion for each
animal. Volume estimations were carried out using the Cavalieri method (Mayhew, 1992). This involved placing a point grid
randomly onto images of spinal cord sections. All images were captured at 4 . All points hitting spinal cord tissue, lesion and artefact
were counted and recorded in Microsoft EXCEL . Volume was calculated for each point group using the following formula:

$V = \Sigma P \cdot A \cdot T$

V = volume, P = number of points hitting region of interest, A = area associated with each point and T = distance between each

sampled section, where area associated with each point = (distance between adjacent points/linear magnification) The proportion of spinal cord occupied by the lesion, i.e. volume fraction (V), was calculated by dividing the volume of the lesion by the volume of the spinal cord less the volume of any artefact present (Howard & Reed, 2005). Mean lesion size ± SE was calculated for each treatment and time point.Stereological analysis was also carried out on immunostained spinal cord sections. For each antibody, four images were captured per section at 20×. The images were captured from random fieldso f view around the edge of the lesion in each animal. A point gridwas again placed randomly on the images captured and the number of points hitting fluorescent structures and the entire field of view were counted and recorded in Microsoft EXCEL . V of the positively immunostained tissue was calculated by dividing the number of points overlying immunoreactive cells by the total number of points hitting tissue. The mean V immunoreactivity ± SE was calculated for each treatment and time point.

Statistics

Statistical calculations were performed using MINITAB software. A two-way analysis of variance was performed to examine effect of time post-injury, treatment and interaction. *Post-hoc* comparisons were undertaken by a Tukey's test. Differences were considered to be statistically significant at a probability value (P) < 0.05.

Results

Lesion size

Calculation of lesion volume involved the application of the Cavalieri principle. The Cavalieri formula was applied to one spinal cord section from each sampling region of all animals. The average volume of the lesion created by the contusion injury in each group was calculated (Fig. 1A). At the 3-week time point, the average lesion volume was found to be 1.03 ± 0.40 mm in the control group and 1.18 ± 0.39 mm in the CsA-treated group. At the 7-week time point the lesion volume in both control (2.27 ± 0.44 mm) and CsA (2.36 ± 0.28 mm) treated groups showed little difference, averaging at 2.3 mm. There was significant increase in size between the 3- and 7-week time points in both control and CsA-treated groups,indicating progressive tissue damage with increasing time post-injury. The V of the lesion was also calculated for each group and time point (Fig. 1B). On average, the control group lesions occupied 2.9% more of the spinal cord volume than the CsA-treated group lesions. No difference in V was observed between the two animal groups at either time point. As before, there was a significantly larger lesion at 7 weeks compared to 3 weeks post-injury when analyzing V of lesion.

Cellular environment of lesion site in injured spinal cord

The V of immunoreactive cells in the sampled images was calculated for both the 3- and 7-week time points (Figs 2 and 5, respectively). There is an obvious circular aggregation of blue DAPI-stained nuclei in the dorsal aspect of the spinal cord identifying the lesioned area (Figs 3, 4, 6 and 7).

Glial scar

In spinal cord-injured tissue the glial scar surrounding the site of lesion mainly comprises astrocytes. V of GFAPpositive astrocytes and vimentin- and BLBP-positive reactive astrocytes at the 3-week time point in control and CsAtreated animals are shown in Figs 3 and 4, respectively.Vimentin and BLBP are normally only seen in radial glia

during CNS development; however, following injury, astrocytes that have become reactive begin to express
these markers as well as GFAP. There are notably more GFAPimmunoreactive astrocytes present in the CsA-treated
group at 3 weeks post-injury (Fig. 2). Fluorescent images show vimentin (Figs 3A, 4A) staining in the entire spinal
cord section. In Figs 3B and 4B, the orange colour shows the overlap of red GFAP and green vimentin staining,
which indicates that there is co-expression of the two antibody markers by the cells in the lesion area. Not all
astrocytes co-express vimentin with GFAP. Vimentin staining around the central canal is not co-localized with GFAP
(Fig. 4A). This ventricular zone region is where adult stem cells are located; these cells normally express vimentin.
Intense orange staining around the margin of the section demonstrates that astrocytes contribute to the glia
limitans. BLBP immunoreactivity was concentrated in the glial scar and although there was less BLBP expression than vimentin surrounding the lesion, the control group again showed significantly less expression of BLBP than the
CsA-treated group (Figs 2, 3C,D). At the 7-week time point there was a significant decrease in the presence of GFAPpositive astrocytes at the lesion site in CsA-treated animals compared to control (Fig. 5). However, no such difference was observed with vimentin- or BLBP-stained cells within both groups of animals at the same time point. GFAPimmunoreactive astrocytes are observed within the lesion centre at this time point (Figs 6A,B, 7A,B). Vimentin and BLBP are found in the scar surrounding the lesion at 7 weeks post-injury (Figs 6B,D, 7B,D).

Neurons

A decrease in NeuN-positive neuronal nuclei was observed in the CsA-treated group compared to control at 3 weeks
post-injury (Fig. 2). Figures 3D and 4D show the interaction between the NeuN-stained neurons and BLBP-stained
astrocytes in control and CsA-treated animals at 3 weeks. Positive NeuN staining is limited to the central grey matter of the spinal cord, with some cells located adjacent to the lesion itself. The BLBP staining is again concentrated
around the lesion, with some processes extending into the lesion itself (Fig. 4D). There was no evidence of any
interaction between the astrocytes and neurons around the lesion. At the 7-week time point there was no difference
between V of neurons stained with NeuN in the lesion environment of either animal group (Fig. 5). Some of
these cells appeared within the BLBP-labeled glial scar tissue (Figs 6D, 7D).

Oligodendrocytes

A decrease in MBP-positive oligodendrocytes was observed in the lesion environment of CsA-treated animals compared to control at 3 weeks post-injury (Fig. 2). MBP may be staining myelin debris which is normally found at the
lesion site following injury. This decrease may reflect a decrease in myelin debris in CsA-treated animals, which
may help regeneration, as myelin debris is one of theinhibitory factors present following injury. There is
widespread positive staining for MBP-expressing oligodendrocytes throughout the white matter (Figs 4E, 5E)
and this staining is also found within the lesion (Figs 4F, 5F) at the 3-week time point. No change in amount of MBP

immunostaining was observed at the 7-week time point (Fig. 5). MBP was again observed within white matter and
in the lesion site (Figs 6E,F, 7E,F). When a comparison between the 3- and 7-week time points is made, the V of cells immunostained with GFAP, vimentin, BLBP and MBP is significantly larger at the 7-week time point compared to 3 weeks. However, there are significantly fewer NeuN-stained neurons at 7 weeks compared to 3 weeks.

SEM analysis of injured environment

Analysis of surface features in spinal cord transverse sections using SEM reveals clusters of rounded cells at the lesion site within untreated animals (Fig. 8A,B,E,F), compared to a more fibrous-appearing environment in CsA-treated animals (Fig. 8C,D,G,H) at both time points. CsA may be providing a fibrous support scaffold that could potentially promote regeneration across the lesion site.

Analysis of collagen in lesioned spinal cord

Masson's trichrome staining reveals green collagen-stained fibres, which are more prevalent in CsA-treated animals
compared to control animals at both time points (Fig. 9). This collagen staining likely corresponds to the fibrous
structures observed with SEM.

Analysis of functional recovery

A two-way analysis of variance of right hindlimb BBB data revealed no significant effect of time after injury, CsA treatment and or interaction between animal groups (Fig. 10A,B). A two-way analysis of variance of left hindlimb
BBB data revealed a significant effect of time after injury ($P< 0.01$), CsA treatment ($P< 0.05$) and no significant interaction (Fig. 10C,D). Subsequent Tukey's tests revealed a significant functional improvement in the CsA group at
the 3-week time point compared to control animals (Fig. 10D). This indicates the effect of CsA on promoting
functional recovery following injury acts only as a shortterm option following injury. It also indicates that during
contusion of the spinal cord, the instrument may not have displaced the spinal cord accurately along the medial
aspect of the spinal cord.

Discussion

In the present study, a marked difference in the cellular environment of the secondary injury was observed in the
CsA-treated group compared to the untreated group. The V of lesion occupying the spinal cord was slightly reduced in the CsA-treated group. However, our findings do not provide a statistically significant difference between the
two groups to determine whether the CsA is an effective neuroprotective agent in terms of reducing lesion volume.
CsA has been reported to possess immunosuppressive and anti-inflammatory properties which serve to reduce
chronic inflammation (Borel, 1991). Therefore, it would be expected that CsA application should reduce the volume
of the lesion. Some ambiguity exists, however, in the findings related to the effectiveness of CsA in reducing
tissue damage following spinal cord injury. Rabchevsky et al. (2001) found that CsA administration did not aid in
reducing tissue damage following contusion spinal cord injury. Our findings support the latter theory as we, too,
did not see significant reduction in tissue damage. CsA treatment has been shown to inhibit lipid peroxidation

and thus contribute to a less inhibitory environment following injury (Diaz-Ruiz et al. 2005). Macrophages have been reported to phagocytose cellular debris (Pizzi & Crowe, 2006) and damaged myelin, which results in an increase in axonal regeneration. Following immune cell infiltration, the next major event in the secondary degeneration
of the spinal cord is the migration of astrocytes to the site of injury, eventually leading to the formation of
the astrocytic glial scar around the lesion. CsA-treated animals displayed a dramatic up-regulation of astrocytes
compared to the control group at 3 weeks post-injury. CsA did not appear to induce cell death of astrocytes as
reported by Pyrzynska et al. (2001). The astrocytes were identified using the markers GFAP, BLBP and vimentin.
The astrocytes present in the lesion core were seen to coexpress GFAP and vimentin, while other astrocytes present
outside the lesion only expressed GFAP. This suggests that there are subgroups of astrocytes which act differently
following spinal cord injury. The GFAP group represents the regular active astrocytes already present in that area of the spinal cord, while the GFAP- and vimentin-expressing group are reactive astrocytes which proliferate and migrate to the site of injury following spinal cord injury. Vimentin is expressed initially during development by immature astrocytes and is re-expressed by reactive astrocytes following spinal cord injury (Pencalet et al. 2006). Similar to the case of macrophages and microglia, reactive astrocytes appear to have a phase-dependent role following spinal cord injury which accounts for seemingly conflicting functions (Okada et al. 2006). The severity of spinal cord injury has been found to be significantly reduced with the presence of reactive astrocytes before completion of the glial scar (Faulkner et al. 2004). This is due to their woundhealing properties, protective properties for neurons and oligodendrocytes, and their ability to limit immune cell migration and inflammation. In this instance, CsA administration seems to have up-regulated astrocyte proliferation at 3 weeks post-injury. However, there is a drawback to this scenario, as the resultant denser astrocytic glial scar acts as a stronger physical barrier through which regenerating axons cannot pass. Once again, a balance must be achieved between the positive and negative effects of CsA administration to ensure optimal tissue preservation and repair. At 7 weeks post-injury, CsA-treated animals show less GFAP immunoreactivity compared to untreated animals, which may aid regeneration through the physical barrier of scar tissue. The latter finding correlates with the findings of López-Vales et al. (2005), who found reduced gliosis in injured spinal cord following treatment with the immunosuppressant drug FK506. Vimentin and BLBP are also markers for radial glia, cells which are present during development of the spinal cord. Many of these cells co-expressed GFAP, suggesting that these are in fact reactive astrocytes, as described above. The aggregation of vimentin-positive, GFAP-negative cells round the central canal concurs with findings that vimentin also labels endogenous adult neural stem cells from part of the ependyma of the central canal (Mori et al. 1990; Okano, 2006). Following spinal cord injury, these cells have been reported to migrate from the central canal to the site of injury (Horky et al. 2006; Ke et al. 2006). Myelin from the adult nervous system is inhibitory to regeneration (Fawcett & Asher, 1999) and is released by disrupted axons and also by the death of oligodendrocytes.The amount of oligodendrocyte apoptosis is high within the area of the glial scar and oligodendrocytes reach their lowest level 8 h post-injury (McTigue et al. 2001; Casella et al. 2006). Previous studies found that by application of another immunosuppressant, FK506, oligodendrocyte survival improved (Nottingham et al. 2002; López-Vales et al. 2005) and microglial activity was inhibited (Guzmán- Lenis et al. 2008) following spinal cord injury. Myelin
debris carrying axon growth inhibitors induces growth cone collapse. The phagocytic cell response within the
injured spinal cord is inefficient, allowing myelin debris to remain for prolonged periods of time following spinal cord injury (Vallières et al. 2006). In this study, MBP may be staining the myelin debris created following damage to
the oligodendrocytes, as MBP immunoreactivity was found within the lesion site. The CsA-treated group expresses less

MBP at 3 weeks post-injury, perhaps due to a reduction in myelin debris. At 7 weeks an increase in MBP immunoreactivity was observed in the CsA-treated group, indicating differentiation of myelinating oligodendrocytes or increase in myelin debris. If the latter is the case, then perhaps the CsA is only beneficial in preventing oligodendrocyte
apoptosis as a short-term solution. CsA administration alone would be a futile exercise unless the neuronal population actually regenerates and reforms synaptic connections. Investigation of the presence of neurons at the site of injury revealed some interesting results. Following spinal cord injury, neuronal death occurs rapidly and within 48 h; only approximately 10% of neurons have been reported to remain at the lesion site (Casella et al. 2006). This rapid loss is probably due to the disruption of the cell membranes from the impact of the injury. We used NeuN to stain for the incidence of neurons. NeuN expression was down-regulated in the CsA-treated group at 3 weeks. This is unexpected as CsA application has been found to preserve neurons following injury by reducing lipid peroxidation (Ibarra et al. 2003). At 7 weeks postinjury, significantly fewer NeuN neurons were present, indicating that the delayed administration of CsA until 4 days post-injury may have limited its effectiveness in fulfilling its neuroprotective role. Analysis of the injured spinal cord using SEM revealed that the architecture of the lesion site within CsA-treated
and untreated groups of animals was very different. A collagenous basement membrane-rich fibrous scar forms
at the lesion site following spinal cord injury (Klapka et al. 2005; Klapka & Müller, 2006). The scar consists of a dense
collagen meshwork, which may serve as a binding matrix for growth-promoting factors. Collagen fibres present within the lesion of CsA animals. The morphology of spinal cord lesion within untreated animals revealed rounded
clusters of cells. Further investigation using markers of apoptosis will determine whether these are in fact dead/
dying cells.Previous experiments investigating the therapeutic effects of CsA following spinal cord injury found that
greatest functional recovery was observed in animals that were administered CsA 6 h post-injury (Diaz-Ruiz et al.
1999). Here we observed functional recovery at 3 weeks post-injury when CsA was administered 4 days following
contusion. Rabchevsky et al. (2001) also failed to see improvement in functional recovery following CsA treatment
15 min post-injury. Our administration of CsA 4 days post-injury may be a more optimal time for administration
as the initial primary wave of injury would have passed. We did not see any functional improvement at 5 and 7
weeks post-injury; this may be because the blood–brain barrier had become impermeable to CsA. There have been
fluctuations in permeability of the blood–brain barrier following injury that may hinder uptake of CsA (Begley
et al. 1990; Sullivan et al. 2005). Although we saw some functional improvement at 3 weeks post-injury, this was
only observed in the left hind limbs, indicating that the damage caused by the contusion may have been centred
slightly toward the right side of the spinal cord, meaning that more axons on the left side of the spinal cord were
perhaps spared. The fact that functional improvement is not always evident following CsA treatment may be linked
to the fact that calcineurin is a key component of the pathways relaying nerve electrical activity and skeletal
muscle growth (Olson & Williams, 2000; Serrano et al. 2001). Inhibition of calcineurin with CsA treatment may
have altered the signalling of hindlimb muscles and in turn affected functional recovery.Currently, methods to treat spinal cord injury are minimal and there is a need to find realistic strategies for

treatment of individuals suffering spinal cord injury.The secondary injury which arises as a result of spinal cord injury provides a major barrier to the repair and regeneration of the spinal cord. However, it is not impenetrable. Due to the fact that the secondary injury occurs over a
period of days and weeks following the initial injury, a therapeutic window is present which gives a chance for
intervention to alter its progression. Previous work has found that the administration of immunosuppressant
drugs within a strict time interval following injury allows for the modulation of astrocytes (Kaminska et al. 2004).
CsA has the properties of a promising drug, an immunosuppressant, with the ability to diminish tissue damage
and also the capability to promote the regeneration of neurons (Ibarra et al. 2003). CsA administration has proven
that the cellular environment of the injured spinal cord can be altered. Further investigation is required to determine
the effect of CsA administration on each component of the cellular environment at different time points post-injury.
Positive results in this respect will create new optimism in the field that an effective strategy to overcome spinal cord
will be achieved.

Acknowledgements
This research was funded by Science Foundation Ireland and the National University of Ireland Galway Millennium Research Fund.
The authors would like to thank Dr Ariella Magee and Ms Eleanor Donnelly for their technical assistance.

Author contribution
Siobhan S. McMahon: Conception and design, Data analysis and interpretation, Manuscript writing. Silke Albermann: Data analysis
and interpretation. Gemma E. Rooney: Data analysis and interpretation. Cathal Moran: Collection and/or assembly of data. Timothy
O'Brien: Final approval of manuscript. Jacqueline Hynes: Data analysis and interpretation. Yolanda Garcia: Collection and/or
assembly of data, Final approval of manuscript. Peter Dockery: Data analysis and interpretation. Anthony J. Windebank: Conception
and design, Final approval of manuscript. Frank P. Barry: Conception and design, Final approval of manuscript.

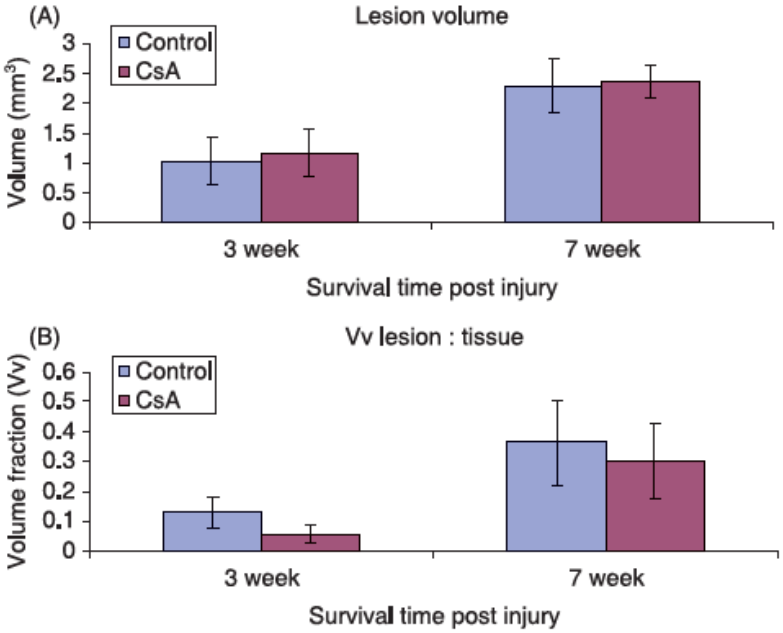

Figure 1 Graphs show (A) volume of lesion and (B) V_v of lesion in CsA-treated and control groups of animals at 3- and 7-week time points. Error bars represent standard error of the mean.

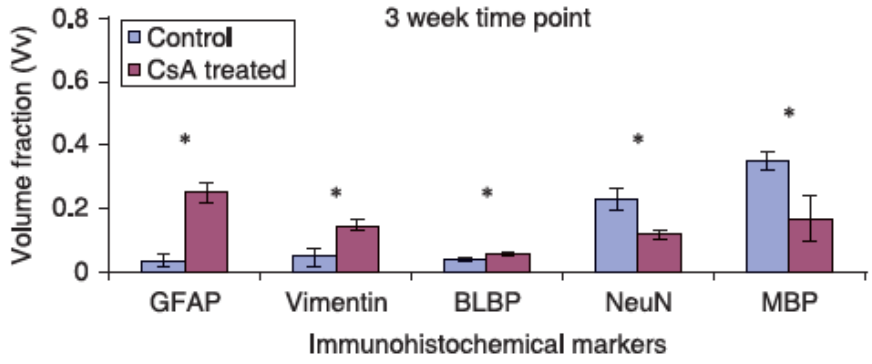

Figure 2 Graphs comparing the V_v of immunoreactive cells in the lesion area at 3 weeks post-injury. This illustrates the proportion of each contributing cell type to the lesion environment in CsA-treated and control groups. Error bars represent standard error of the mean. *$P < 0.05$.

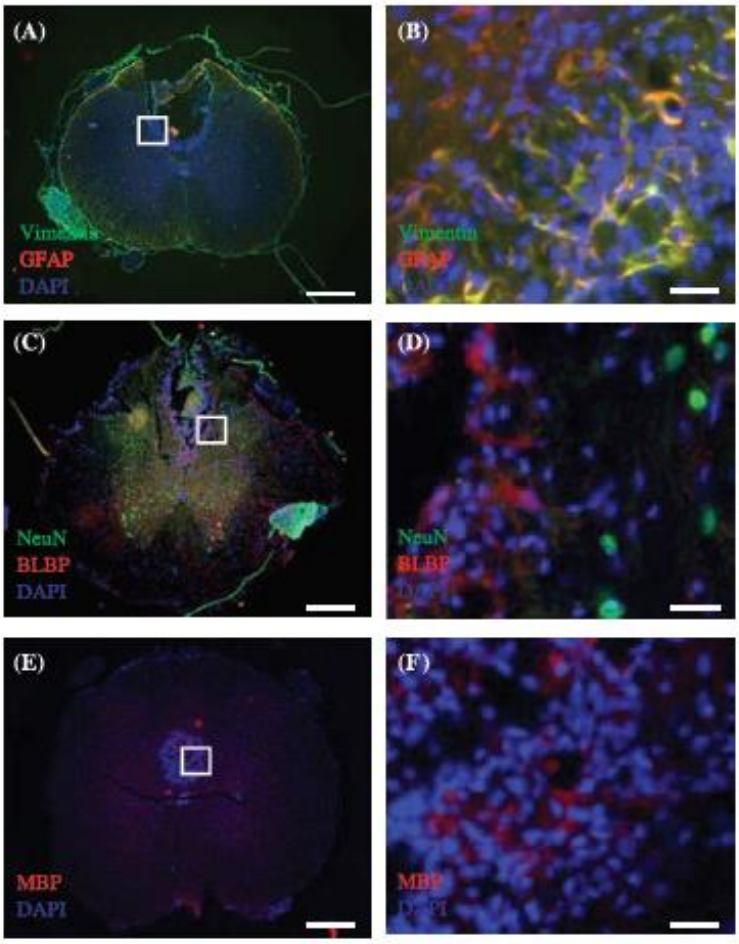

Figure 3 Merged images of immunohistochemically stained transverse sections of injured spinal cord tissue taken from control group at 3 weeks post-injury. (A,B) Vimentin (green) and GFAP (red) immunoreactive cells. Region within white box in (A) is shown in (B). (C,D) BLBP (red) and NeuN (green) immunoreactive cells. (E,F) MBP (red) immunoreactive cells. Regions within white boxes in (A,C,E) are shown in (B,D,F), respectively. DAPI (blue) counterstain was used to label cell nuclei in all images. Scale bars: (A,C,E) 500 µm, (B,D,F) 30 µm.

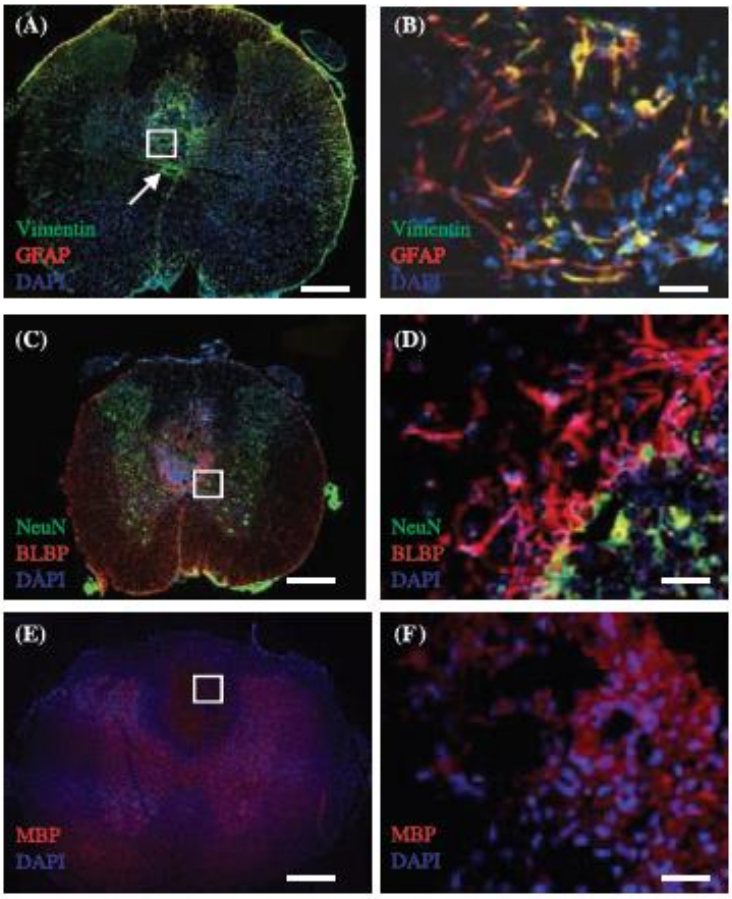

Figure 4 Merged images of immunohistochemically stained transverse sections of injured spinal cord tissue taken from CsA-treated group at 3 weeks post-injury. (A,B) Vimentin (green) and GFAP (red) immunoreactive cells. The orange colour around the edge of the section shows that astrocytes contribute to the glia limitans. Some orange is also observed around the lesion. Expression of vimentin-positive, GFAP-negative staining around the central canal is obvious in (A). Region within white box in (A) is shown in (B). Arrow in (B) shows central canal of spinal cord. (C,D) BLBP (red) and NeuN (green) immunoreactive cells. Most BLBP positive astrocytes are located in region of glial scar, whereas NG2 positive cells are located within lesion. NeuN staining shows the dispersion of neuronal nuclei in the spinal cord section with an obvious concentration in the grey matter. (E,F) MBP (red) immunoreactive cells. MBP staining shows the dispersion of oligodendrocytes in the spinal cord section with obvious staining within the lesion which may relate to myelin debris that persisted following injury. Regions within white boxes in (A,C,E) are shown in (B,D,F), respectively. DAPI (blue) counterstain was used to label cell nuclei in all images. Scale bars: (A,C,E) 500 µm, (B,D,F) 30 µm.

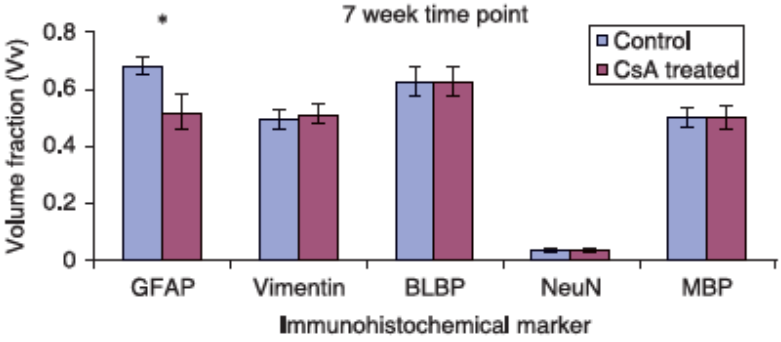

Figure 5 Graphs comparing the V_v of immunoreactive cells in the lesion area 7 weeks post-injury. Error bars represent standard error of the mean. $^*P < 0.05$.

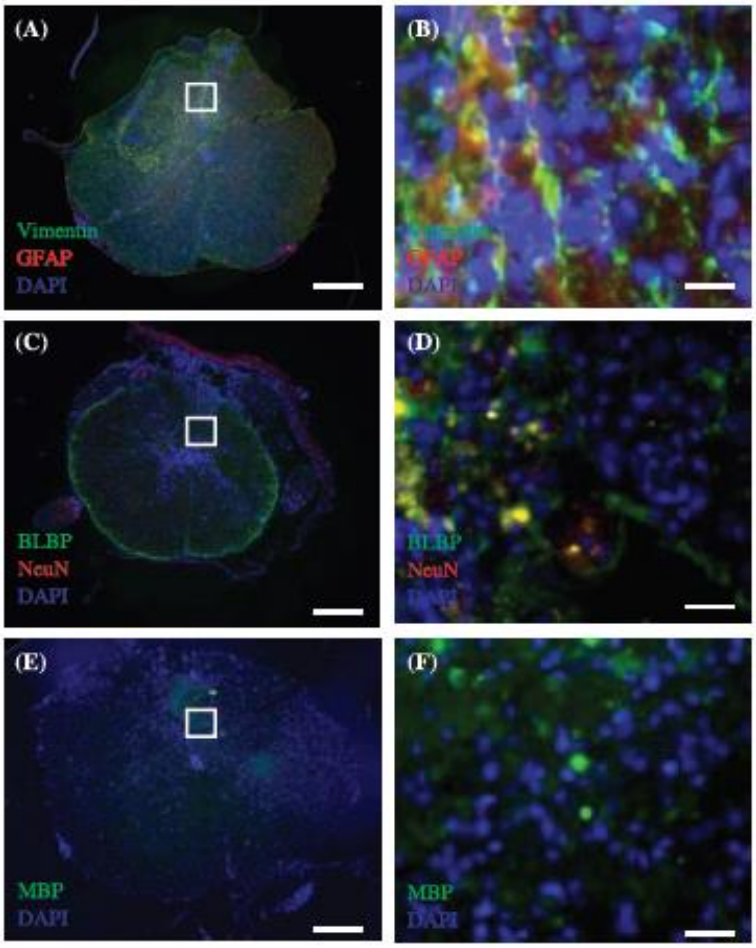

Figure 6 Merged images of immunohistochemically stained transverse sections of injured spinal cord tissue taken from control group at 7 weeks post-injury. (A,B) Vimentin (green) and GFAP (red) immunoreactive cells. (C,D) NeuN (red) and BLBP (green) immunoreactive cells. (E,F) MBP (green) immunoreactive cells. Regions within white boxes in (A,C,E) are shown in (B,D,F), respectively. DAPI (blue) counterstain was used to label cell nuclei in all images. Scale bars: (A,C,E) 500 µm, (B,D,F) 30 µm.

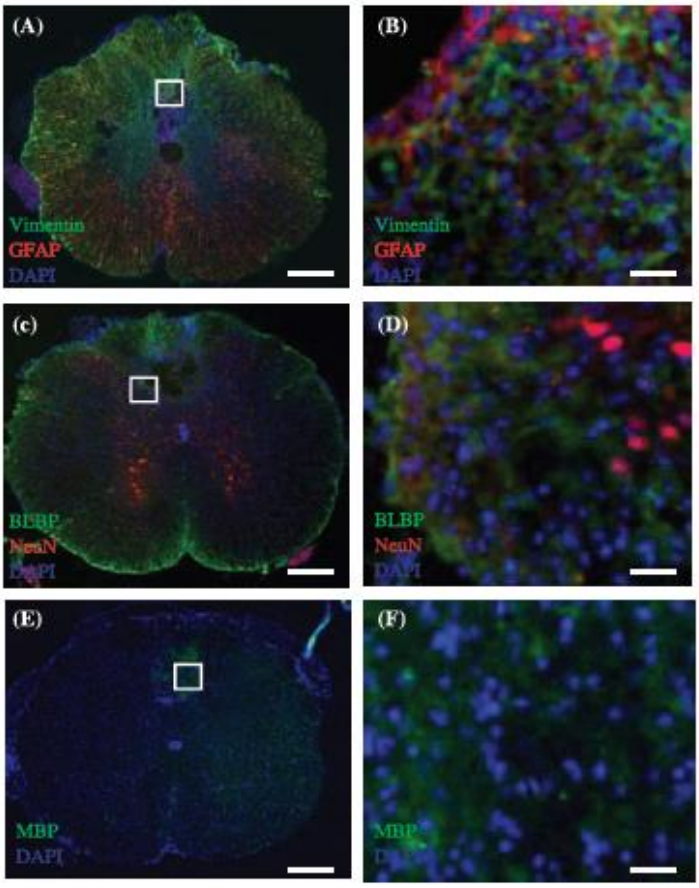

Figure 7 Merged images of immunohistochemically stained transverse sections of injured spinal cord tissue taken from CsA-treated group at 7 weeks post-injury. (A,B) Vimentin (green) and GFAP (red) immunoreactive cells. Astrocytes are evident both surrounding and within the lesion centre. (C,D) NeuN (red) and BLBP (green) immunoreactive cells. NeuN staining is limited to grey matter. (E,F) MBP (green) immunoreactive cells. Regions within white boxes in (A,C,E) are shown in (B,D,F), respectively. DAPI (blue) counterstain was used to label cell nuclei in all images. Scale bars: (A,C,E) 500 µm, (B,D,F) 30 µm.

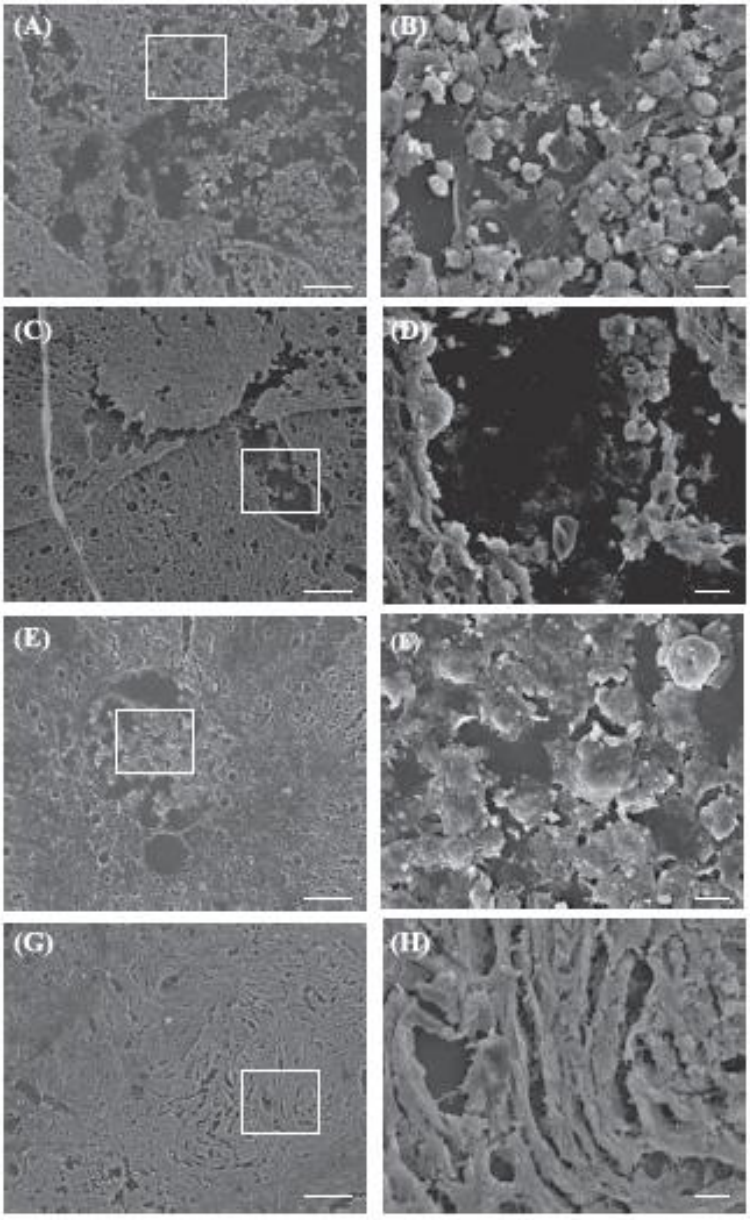

Figure 8 SEM images show spinal cord transverse sections in 3-week control (A,B) and CsA-treated group (C,D), and in 7-week control (E,F) and CsA-treated group (G,H). Regions within white boxes in (A,C,E) are shown in (B,D,F), respectively. Scale bars: 100 μm.

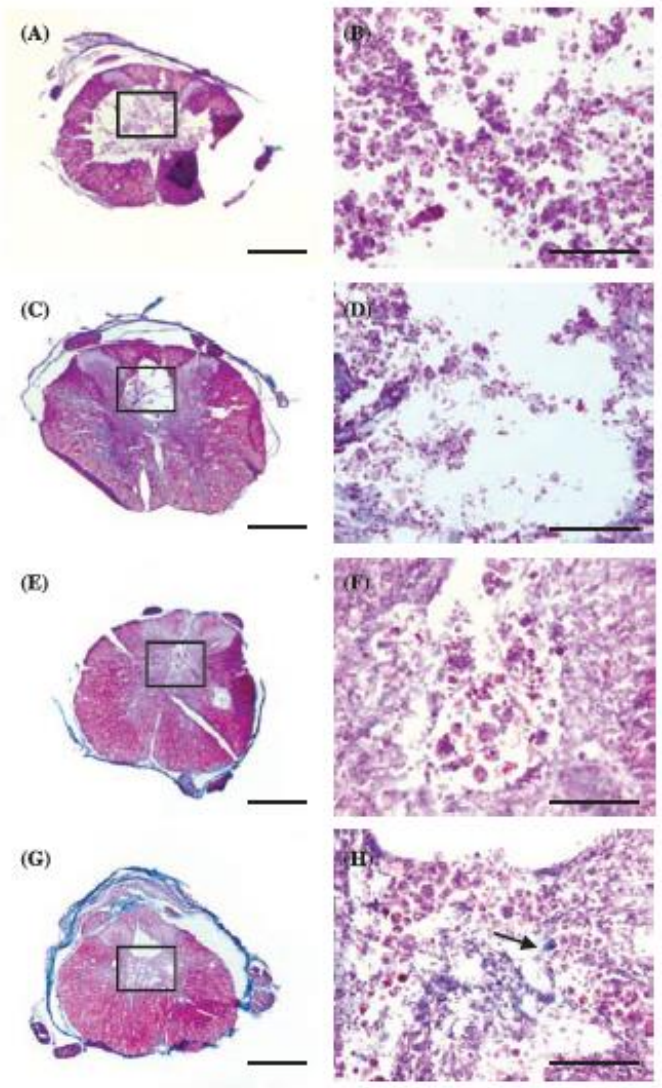

Figure 9 Light microscopy images show Masson's trichrome staining on spinal cord transverse sections in 3-week control (A,B) and CsA-treated group (C,D), and in 7-week control (E,F) and CsA-treated group (G,H). Regions within white boxes in (A,C,E) are shown in (B,D,F), respectively. Arrow points to collagen (green) fibres. Scale bars: 100 μm.

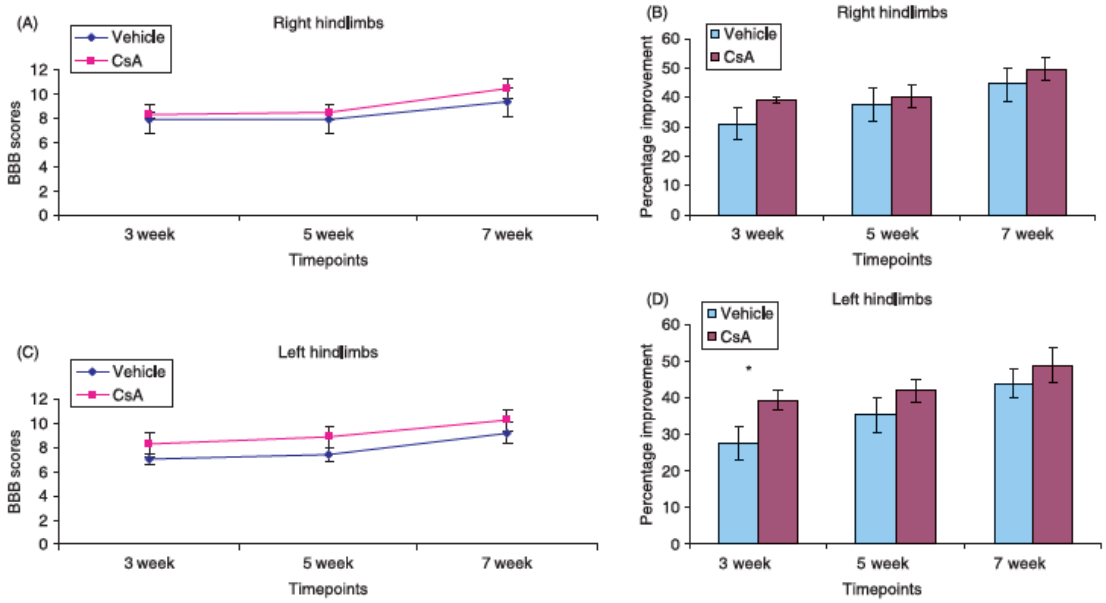

Figure 10 Graphs show BBB scores (A,C) and percentage improvement of BBB scores (B,D) in right and left hindlimbs, respectively, of animals in control and CsA-treated groups at 3, 5 and 7 weeks post-injury. Error bars represent standard error of the mean. $*P < 0.05$.